International Journal of Statistics and Applied Mathematics 2023; 8(5): 25-30

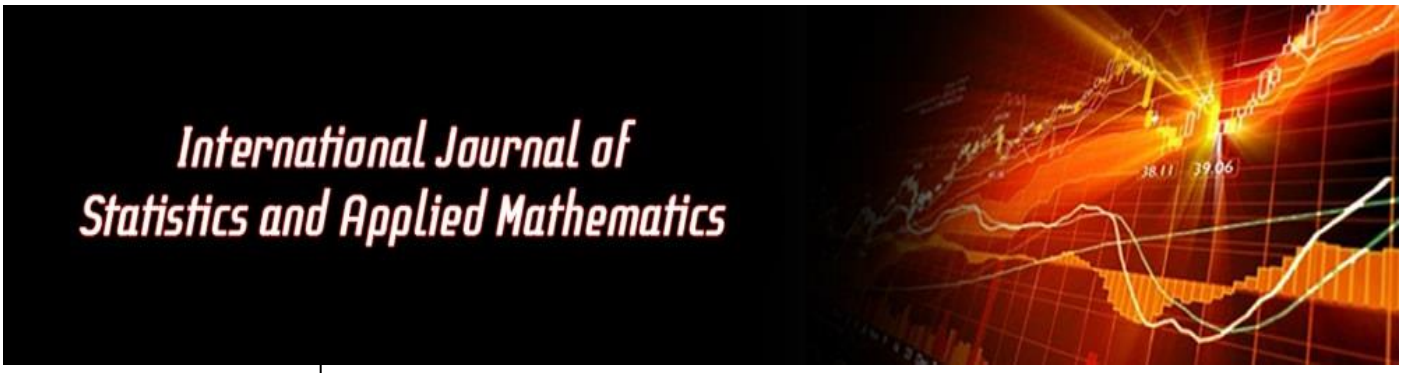

ISSN: 2456-1452
Maths 2023; 8(5): 25-30

https://www.mathsjournal.com
Received: 11-07-2023
Accepted: 16-08-2023

M Yasin
An-Najah National University, Nablus, Palestine

H Hamad
An-Najah National University, Nablus, Palestine

F Aqel
An-Najah National University, Nablus, Palestine

Y Jaafra
An-Najah National University, Nablus, Palestine

Corresponding Author:
M Yasin
An-Najah National University, Nablus, Palestine

Radial basis functions for solving Volterra integral equations

M Yasin, H Hamad, F Aqel and Y Jaafra

Abstract
In this paper, Radial Basis Functions (RBFs) Interpolation is used for the solution of Volterra integral equations of the first kind. We used three types of RBFs: Inverse Multiquadric, Multiquadric and Gaussian. The goal of this work is to verify the effectiveness of the method on solving the Volterra integral equation of the first kind numerically. Moreover, we look into the possibility of the convergence of the method by increasing the number of center points. This investigation is done by studying three different examples verifying the performance of the method and showing the behavior of error using the Root-Mean-Square-Deviation (RMSD). Finally, the results show that the Gaussian has superiority over the Multiquadric and Inverse Multiquadric radial basis functions.

Keywords: Radial basis functions, interpolation, approximation, first kind Volterra equation, integral equation

1. Introduction
Volterra integral equations have received huge attention in recent years, as these equations are involved in many scientific fields, such as engineering, economics, and medicine [10, 14]. This led interested people to study these equations analytically as well as produce numerical methods to solve these equations. The general form of the linear Volterra integral equation of the first kind is

$$\int_0^{\infty} K(x,s)y(s)ds = g(x), 0 \leq s \leq x \leq 1, \quad (1)$$

Where $g(x): \mathcal{R} \to \mathcal{R}$ is the input function and $K(x,s): \mathcal{R} \times [0,1] \to \mathcal{R}$ is a kernel function, where both g and K are given functions, while $y(x)$ is the unknown function. In literature, equation (1) was solved numerically using several methods. The authors in [11] used a modification of Block Pulse Functions to solve equation (1). A recent work in [7] used the Swai Decomposition method to solve Volterra integral equations. Khidir in [9] presented a numerical technique based on the Chebyshev Spectral method for solving Volterra integral equations. Saberi *et al.* [13] approximated solutions of linear Volterra equations by applying the Wavelet-Galerkin scheme. Another direction for solving Volterra integral equations numerically is the radial basis functions interpolation approach; which approximates the solution on some given points that have no particular structure, for example authors in [1] used a mesh-less method for approximating solutions of Fredholm and mixed Volterra-Fredholm integral equations. Authors in [4, 5] have presented methods based on RBFs and iterative procedures for the solution of Fredhom and Volterra integral equations. In [3], authors used RBFst to solve different types of integral equations, moreover, they showed that this method has an exponential convergence rate. Finally, Zhang *et al.* in [15] proposed a radial basis functions method focusing on the multiquadric function for solving some integral equations. The authors compared their results with the thin plate spline method and Haar wavelet method showing the Multiquadric method gives better accuracy.
In this work, the Volterra integral equation is numerically solved by using several types of radial basis functions.

The structure of this paper is as follows: after this introduction, radial basis functions are introduced in Section 2. The RBF interpolation method is presented in Section 3. In Section 4, numerical examples are performed. Finally, Section 5 is devoted to the conclusion.

Radial Basis Functions

Radial Basis Functions were introduced in the year 1971, Hardy was the first one to develop and implement the RBFs to interpolate multidimensional scattered data, and indeed he tried to use it to approximate the earth's gravitational field [6]. Radial basis function $\Phi: \mathcal{R}^d \to \mathcal{R}$, d is a positive integer, is defined as a function of distance $r = \| x - t_i \|$, where $\|.\|$ is the Euclidian norm and ti is called the centers. Then an approximation of a function $y(x)$, denoted by $\hat{y}(x)$, using radial basis function is given as in the following formula:

$$y(x) \approx \hat{y}(x) = \sum_{i=1}^{N} \alpha_i \phi(\| x - t_i \|), \quad (2)$$

where α_i are coefficient numbers and $\phi(r)$ is the radial basis function. Some commonly known RBFs are illustrated in Table 1.

Table 1: A set of common RBFs.

Name of RBF	$\phi(r), (r \geq 0)$
Inverse multiquadric (IMQ)	$\phi(r) = \frac{1}{\sqrt{1+(\varepsilon r)^2}}$
multiquadric (MQ)	$\phi(r) = \sqrt{1+(\varepsilon r)^2}$
Gaussian (GA)	$\phi(r) = e^{-(\varepsilon r)^2}$

To find the coefficients α_i, consider a set of distinct points $x = \{x_1, x_2, \ldots, x_N\}$ and a corresponding data values $\boldsymbol{w} = \{w_1, w_2, \ldots, w_N\}$, substituting in (2) gives a system that can be written in a matrix form,

$$A\boldsymbol{\alpha} = \boldsymbol{w},$$

Where

$$A = \begin{bmatrix} \phi_{11} \phi_{12} \cdots \phi_{1N} \\ \phi_{21} \phi_{22} \cdots \phi_{2N} \\ \vdots \quad \vdots \quad \ddots \quad \vdots \\ \phi_{N1} \phi_{N2} \cdots \phi_{NN} \end{bmatrix}, \phi_{ji} := \phi(\|x_j - t_i\|), i, j = 1, 2, \ldots, N. \quad (4)$$

Indeed, the linear system (3) can be solved for $\boldsymbol{\alpha}$ as the coefficient matrix A is nonsingular, because the RBFs considered here are sufficiently smooth, see for instance [8]. Therefore, solving system (3) gives:

$$\boldsymbol{\alpha} = A^{-1}\boldsymbol{w}. \quad (5)$$

Description of the method

We consider the first kind of Volterra integral equation defined by,

$$\int_0^x K(x,s) y(s) ds = g(x), 0 \leq s \leq x, \quad (6)$$

where $y(x)$ is the function being sought, $K(x,s)$ and $g(x)$ are two given C^{∞} functions with $g(0) = 0$. In the following, a numerical method based on using radial basis functions interpolation is used to get an approximating solution to equation (6). To start, take N points $(t_1, t_2, \ldots, t_N)$ in the interval $[0,1]$, suchpoints are called center points. Then the solution $y(x)$ of equation (6) can be approximated by writing it as a linear combination of N RBFs:

$$y(x) \approx \hat{y}(x) = \sum_{i=1}^{N} \alpha_i \boldsymbol{\Phi}_i(x) \quad (7)$$

Where $\hat{y}(x)$ is the approximate solution, $\alpha_i's$ are constant coefficients and $\boldsymbol{\Phi}_i(x) := \phi(||x - ti||)$ are smooth radial basis functions some of which are defined in Table1. Substituting the linear combination (7) in equation (6) gives:

$$\int_0^x K(x,s) \sum_{i=1}^{N} \alpha_i \boldsymbol{\Phi}_i(s)\, ds \approx g(x) \quad (8)$$

The linear property of integrals implies,

$$\sum_{i=1}^{N} \alpha_i \int_0^x K(x,s) \boldsymbol{\Phi}_i ds \approx g(x) \quad (9)$$

Now, substituting a set of collocation points $x_j \in [0,1], j = 1, 2, \ldots N$ in equation (9) gives the system,

$$\sum_{i=1}^{N} \alpha_i \int_0^{x_j} K(x_j, s) \boldsymbol{\Phi}_i ds = g(x_j), j = 1, 2, \ldots N \quad (10)$$

Let K denote the $N \times N$ matrix,

$$\boldsymbol{K} := \begin{bmatrix} K_{11} K_{12} \cdots K_{1N} \\ K_{21} K_{22} \cdots K_{2N} \\ \vdots \quad \vdots \quad \ddots \quad \vdots \\ K_{N1} K_{N2} \cdots K_{NN} \end{bmatrix},$$

Where

$$K_{ij} := \int_0^{x_j} K(x_j, s) \Phi_i(s) ds.$$

In the numerical implementation performed later, Gauss Quadrature method used to approximate the definite integrals K_{ij} as follows,

$$K_{ij} := \int_0^{x_j} K(x_j, s) \Phi_i(s) ds = \frac{x_j}{2} \int_{-1}^{1} K\left(x_j, Q(z)\right) \Phi_i\big(Q(z)\big) dz \approx \sum_{r=1}^{R} m_r K\big(x_j, Q(z_r)\big) \boldsymbol{\Phi}_i\big(Q(z_r)\big). \quad (12)$$

Where $Q(z) := \frac{x_j}{2} + \frac{x_j z}{2} = s$ and m_r is the weight of the integral approximation. Then the system in (10) can be rewritten in matrix form as,

$$\begin{bmatrix} K_{11} K_{12} \cdots K_{1N} \\ K_{21} K_{22} \cdots K_{2N} \\ \vdots \quad \vdots \quad \ddots \quad \vdots \\ K_{N1} K_{N2} \cdots K_{NN} \end{bmatrix} \begin{bmatrix} \alpha_1 \\ \alpha_2 \\ \vdots \\ \alpha_N \end{bmatrix} = \begin{bmatrix} g_1 \\ g_2 \\ \vdots \\ g_N \end{bmatrix} \quad (13)$$

The system in (13) is solved for α i as follows,

$$\begin{bmatrix} \alpha_1 \\ \alpha_2 \\ \vdots \\ \alpha_N \end{bmatrix} = \begin{bmatrix} K_{11} K_{12} \cdots K_{1N} \\ K_{21} K_{22} \cdots K_{2N} \\ \vdots \quad \vdots \quad \ddots \quad \vdots \\ K_{N1} K_{N2} \cdots K_{NN} \end{bmatrix}^{-1} \begin{bmatrix} g_1 \\ g_2 \\ \vdots \\ g_N \end{bmatrix} \quad (14)$$

Finally, the solution $y(x)$ in (7) becomes,

$$y(x) \approx \hat{y}(x) = [\phi_1(x) \phi_2(x) \ldots \phi_N(x)] \begin{bmatrix} K_{11} K_{12} \cdots K_{1N} \\ K_{21} K_{22} \cdots K_{2N} \\ \vdots \quad \vdots \quad \ddots \quad \vdots \\ K_{N1} K_{N2} \cdots K_{NN} \end{bmatrix}^{-1} \begin{bmatrix} g_1 \\ g_2 \\ \vdots \\ g_N \end{bmatrix} \quad (15)$$

Error analysis and convergence

Define the operator

$$V\,[y(x)] \coloneqq \int_0^x K(x,s)y(s)ds, \qquad (17)$$

that maps continuous functions $y(x)$ to $C(\mathcal{R})$. Consequently, equation (1) becomesin operator form as:

$$V[y] = g \qquad (18)$$

This is a contraction operator since K is a C^{∞} function and $y(x)$ is a continuous solution on a bounded domain which implies a bounded operator, then a simple scaling argument gives the contraction. The Banach contraction mapping principle implies the existence of a unique solution to equation (1). Moreover, the operator V is one-to-one and onto with bounded inverse as a result of the Geometric Series Theorem (See [2], Appendix A).

Let us now put the linear combination of the RBFs in equation (7) in the operator form as a collocation projection operator defined by

$$\mathcal{g}_N[y(x)]: = \sum_{i=1}^{N} \alpha_i \boldsymbol{\Phi}_i(x), \qquad (18)$$

which maps functions from $C(D)$ to span$\{\Phi_1, \Phi_2, \ldots, \Phi_N\} \subset C(\mathcal{R})$. Finally, the integral approximations in (12) are used to introduce the numerical integral operators I_N:

$$I_N[y(x)]: = \sum_{r=1}^{R_N} m_r K\big(x, Q(z_r)\big) y\big(Q(z_r)\big), N \geq 1. \qquad (19)$$

Using the operators above together we can rewrite the problem in the abstract form:

$$\mathcal{g}_N I_N[\hat{y}_N] = g \qquad (20)$$

In the following, we sketch the proof for error analysis and convergence of the RBFs method

- First, the L^{∞} bound of the iterated discrete collocation solution is obtainedassuming that $\mathcal{g}_N[y] \to y$ as $N \to \infty$. See the complete result in ([1], Theorem 4.1).
- Then, the error bound and convergence of the approximate solution $\hat{y}_N$ in (20) can be proved by showing that the L^{∞} distance between $\hat{y}_N$ and the unique solution of the problem is convergent to zero. For a complete result and full details, the reader can refer to ([1], Theorem 4.2).
- From the computations done in ([1], Theorem 4.2) one can see that there are two main errors that are caused by the RBF interpolation and by performing the numerical integration scheme and both errors are bounded. Finally, as the error of the RBF interpolation is dominated over the integration error, then increasing the number of nodes in the numerical integration method has no significant effect on the error.

Numerical results

This section is devoted to testing the method presented above by implementing it through three different examples. Furthermore, error analysis for each example presented by using the Root-Mean-Square deviation (RMSD) defined by,

$$RMSD = \sqrt{\frac{\sum_{i=1}^{N}(y(xi)-\hat{y}(xi))^2}{N}} \qquad (21)$$

In the implementations, we consider three different types of RBFs: Inverse Multiquadric, and Gaussian functions given in Table 1. We aim in this section to study the performance of the presented method by considering the main factors that can affect the behavior of the error which are:

1. The number of center and collocation points N used to build the approximation solution in (15).
2. The number of testing points$M$.
3. The shape parameter ϵ; the optimal choice of ϵ is still under intensive investigation, for more details see [12].

In the following, three different examples are presented for different values of N and M with ϵ = 0.3.

Example 1. Consider the Volterra integral equation

$$\int_0^x (x^2 - s + 2)y(s)ds = (x^2 - x + 2)sin(x) + 1 - cos(x), 0 \leq x \leq 1,$$

Which has the exact solution $y(x) = cos(x)$. For this example, the center and collocation points N are chosen to be the same. Table 2 shows results for exact and approximating solutions with RMSD for different RBFs with$h = 0.2$. These results are represented graphically in Figure 1. Tables 3 and 4 show the RMSD error for different values of, and different numbers of testing points M, respectively. In particular, Table 3 gives an insight into the convergence of the approximating solution of the method to the exact solution $y(x)$. Table 4 shows that the accuracy of the approximating solution $\hat{y}$ increases as the number of testing points M gets larger.

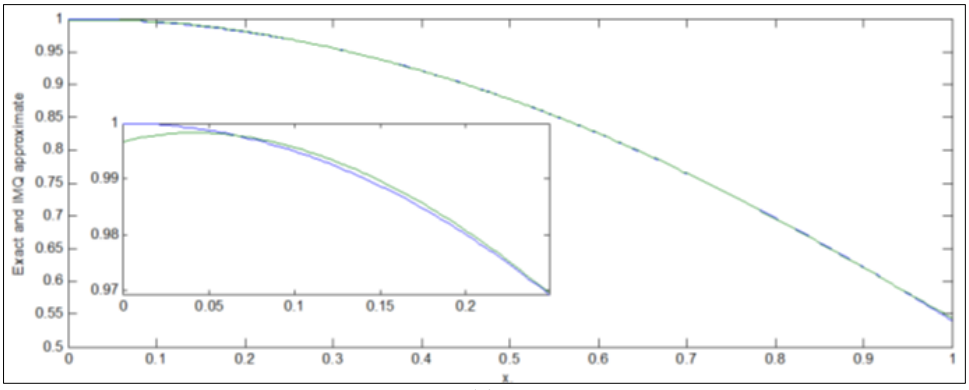

(a)

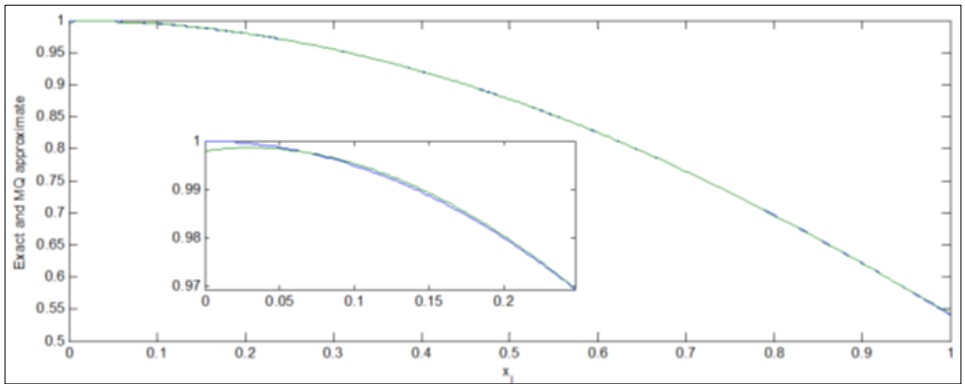

(b)

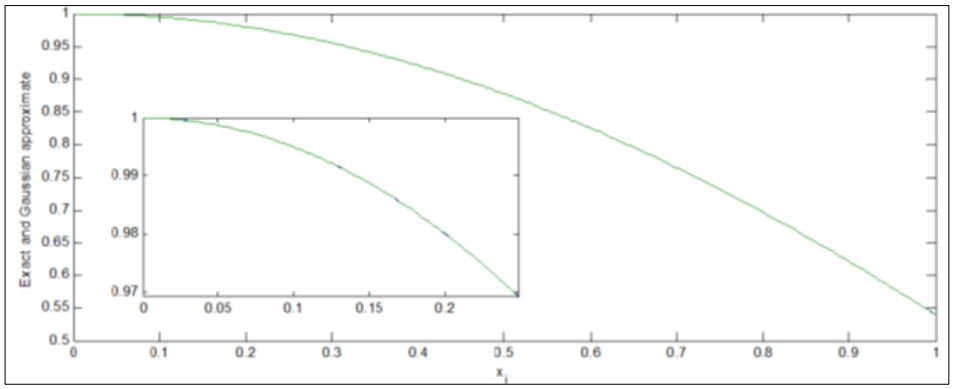

(c)

Fig 1: Exact and the approximating solutions using (a) IMQ,(b) MQ and (c)GA RBFs, respectively, for Example 1

Table 2: Exact and approximating solutions with RMSD results for Example 1.

x_i	$Exact\ y(xi)$	$IMQ\ \hat{y}(x_i)$	$MQ\ \hat{y}(x_i)$	$GA\ \hat{y}(x_i)$
0	1	0.9967524	0.9980215	0.9999740
0.2	0.9800665	0.9807565	0.9804851	0.9800682
0.4	0.9210609	0.9206962	0.9208468	0.9210557
0.6	0.8253356	0.8256994	0.8255556	0.8253349
0.8	0.6967067	0.6959721	0.6962713	0.6966992
1.0	0.5403023	0.5438255	0.5424308	0.5403220
	RMSD	8.2655E-004	4.9919E-04	6.1857E-06

Table 3: RMSD for different values of h for Example 1.

h	RMSD IMQ	RMSD MQ	RMSD GA
0.25	8.6195E-004	8.9512E-004	5.1235E-004
0.20	6.3327E-004	6.5629E-004	7.7655E-005
0.15	7.3499E-005	5.2081E-004	1.1971E-005
0.10	4.4944E-005	4.7546E-004	2.8656E-006
0.05	1.1286E-005	2.2240E-005	1.9435E-006

Table 4: RMSD for different number of testing points M and h for Example 1.

h	M	RMSD IMQ	RMSD MQ	RMSD GA
0.25	50	6.7150E-004	1.5920E-003	8.2445E-005
	100	6.3363E-004	1.5015E-003	7.7701E-005
	200	6.1537E-004	1.4579E-003	7.5412E-005
	400	6.0642E-004	1.4365E-003	7.4290E-005
0.15	50	9.2110E-005	4.9929E-004	2.4352E-006
	100	8.6094E-005	4.9573E-004	2.3407E-006
	200	8.3148E-005	4.9403E-004	2.2949E-006
	400	8.1691E-005	4.9321E-004	2.2723E-006
0.05	50	7.5692E-005	7.9800E-005	9.4324e-007
	100	7.5371E-005	7.3865E-005	9.4235e-007
	200	7.5218E-005	7.0950E-005	9.4055e-007
	400	7.5144E-005	6.9507E-005	9.3677E-007

For the following two examples, similar tables (Tables: 5, 6) as Table 4 of Example 1 are performed which give similar results for different choices of the kernel $K(x,s)$ and $g(x)$.

Example 2. Consider the Volterra integral equation

$$\int_0^x (x-s)y(s)\,ds = 2 + x - 2e^x + xe^x, 0 \le x \le 1.$$

The exact solution of this equation is $y(x) = xe^x$. The numerical results are shown in Table 5.

Example 3. Consider the Volterra integral equation

$$\int_0^x 3^{x-s}y(s)\,ds = x, 0 \le x \le 1.$$

The exact solution is$y(x) = 1 - x\,ln(3)$. The numerical results are shown in Table 6.

Table 5: RMSD for different number of testing points M and h for Example 2.

h	M	RMSD IMQ	RMSD MQ	RMSD GA
0.25	50	1.7635E-002	1.3761E-002	8.5645E-003
	100	1.6737E-002	1.3060E-002	8.1228E-003
	200	1.6295E-002	1.2714E-002	7.9051E-003
	400	1.6075E-002	1.2542E-002	7.7971E-003
0.15	50	2.5007E-003	2.6814E-003	1.8066E-003
	100	2.3461E-003	2.5336E-003	1.7070E-003
	200	2.2700E-003	2.4607E-003	1.6580E-003
	400	2.2323E-003	2.4246E-003	1.6336E-003
0.05	50	5.4858E-005	7.9742E-005	4.2817E-005
	100	5.2899E-005	7.1559E-005	3.8842E-005
	200	5.1975E-005	6.7567E-005	3.6905E-005
	400	5.1530E-005	6.5600E-005	3.5951E-005

Table 6: RMSD for different number of testing points M and h for Example 3.

h	M	RMSD IMQ	RMSD MQ	RMSD GA
0.25	50	9.9480E-005	1.7843E-003	1.9735E-005
	100	9.3132E-005	1.7836E-003	1.8543E-005
	200	9.0057E-005	1.7833E-003	1.7970E-005
	400	8.8547E-005	1.7831E-003	1.7690E-005
0.15	50	6.4504E-005	6.5779E-004	1.6840E-005
	100	6.4509E-005	6.2032E-004	1.5742E-005
	200	6.4512E-005	6.0224E-004	1.5202E-005
	400	6.4514E-005	5.9338E-004	1.4934E-005
0.05	50	2.2422E-005	2.7240E-004	2.4551E-006
	100	2.2027E-005	2.7238E-004	2.4533E-006
	200	2.1849E-005	2.7237E-004	2.4525E-006
	400	2.1764E-005	2.7236E-004	2.4521E-006

Conclusion

In this work, a numerical method is used to solve linear Volterra integral equations of the first kind based on radial basis functions. To verify the efficiency of the presented method, the RMSD error is studied through three different examples. Moreover, the convergence of the approximating solution is tested for variant values of h and showed a stable behavior as h decreased. Finally, while comparing the performance of the implemented RBFs it can be concluded that the Gaussian outperformed the MQ and IMQ RBFs.

References

1. Assari P, Adibi H, Dehghan M. A numerical method for solving linear integral equations of the second kind on the non-rectangular domains based on the mesh less method. Applied Mathematical Modelling. 2013;37(22):9269‑9294.
2. Atkinson K. The Numerical Solution of Integral Equations of the Second Kind. Cambridge University Press; c1997.
3. Avazzadeh Z, Heydari M, Chen W, Loghmani GB. Exponential convergence for numerical solution of integral equations using radial basis functions. Journal of Applied Mathematics; c2014.
4. Golbabai A, Seifollahi S. An iterative solution for the second kind integral equations using radial basis functions. Applied mathematics and computation. 2006;181(2):903‑907.
5. Golbabai A, Seifollahi S. Numerical solution of the second kind integral equations using radial basis function networks. Applied Mathematics and computation. 2006;174(2):877‑883.
6. Hardy RL. Multiquadric equations of topography and other irregular surfaces. Journal of geophysical research. 1971;76(8):1905-1915.
7. Higazy M, Aggarwal S, Nofal TA. Sawi decomposition method for Volterra integral equation with application. Journal of Mathematics; c2020.
8. Jakobsson S, Andersson B, Edelvik F. Rational radial basis function interpolation with applications to antenna design. Journal of computational and applied mathematics. 2009;233(4):889‑904.
9. Khidir AA. A new numerical technique for solving Volterra integral equations using Chebyshev spectral method. Mathematical Problems in Engineering; c2021.

10. Kythe P, Puri P. Computational methods for linear integral equations. Springer Science & Business Media; c2011.
11. Maleknejad K, Rahimi B. Modification of block pulse functions and their application to solve numerically Volterra integral equation of the first kind. Communications in Nonlinear Science and Numerical Simulation. 2011;16(6):2469‑2477.
12. Michael Mongillo *et al*. Choosing basis functions and shape parameters for radial basis function methods. SIAM undergraduate research online. 2011;4(190-209):2‑6,.
13. Saberi-Nadjafi J, Mehrabinezhad M, Akbari H. Solving Volterra integral equations of the second kind by the wavelet-Galerkin scheme. Computers& Mathematics with Applications, 2012;63(11):1536‑1547.
14. Abdul-Majid W. Linear and nonlinear integral equations, Springer; c2011. p. 639
15. Zhang H, Chen Y, Nie X. Solving the linear integral equations based on radial basis function interpolation. Journal of Applied Mathematics; c2014.